Hindawi
Journal of Nanomaterials
Volume 2020, Article ID 2535019, 8 pages
https://doi.org/10.1155/2020/2535019

Research Article

Fast Synthesis of Co_3O_4 by Microwave-Assisted Hydrothermal Treatment

Midilane S. Medina, Alessandra Zenatti, and Marcia T. Escote

Centro de Engenharia, Modelagem e Ciências Sociais Aplicadas, Universidade Federal do ABC, Av. dos Estados 5001, Santo André, SP 09210-580, Brazil

Correspondence should be addressed to Marcia T. Escote; marcia.escote@ufabc.edu.br

Received 26 November 2018; Revised 4 February 2019; Accepted 25 September 2019; Published 4 January 2020

Academic Editor: Muhammet S. Toprak

This work describes a fast and simple procedure that combines the virtues of the microwave-assisted hydrothermal method with an oxidizing agent to produce Co_3O_4 nanocubes and nanoplates. We observed that particle morphology and size depend on the synthesis time and oxidizing agent (urea and hydrogen peroxide). The X-ray diffraction results showed that the samples are single phase, with crystallite sizes of approximately 30 nm. A similar crystalline domain is observed in the transmission electronic images. Magnetic measurements revealed the influence of the size and morphology of the particles on the magnetic curves. These measurements on the nanoplate samples revealed a paramagnetic behaviour at higher temperatures, and the presence of a cusp at that temperature was defined as T_P. The T_P decreases from 36 K to 21 K when the size of the plate particles decreases from ~70 nm to 10 nm. These samples also present weak ferromagnetism below T_P, which is attributed to a superparamagnetic blockade state. The nanocube samples have a lower magnetic susceptibility magnitude and weak ferromagnetism behaviour at room temperature. Our results show that this synthesis produces Co_3O_4 nanoplates and nanocubes with interesting magnetic properties related to their shape and size.

1. Introduction

Co_3O_4 is a useful material for many technological applications, including ion-lithium batteries [1], gas sensors [2], and supercapacitors [3]. The magnetism of Co_3O_4 has also attracted much attention because nanostructured Co_3O_4 exhibits antiferromagnetism and superparamagnetism [4].

Bulk Co_3O_4 presents antiferromagnetic (AFM) ordering with a Néel temperature, T_N, of approximately 40 K [5]. However, some studies have reported a reduction in T_N values and superparamagnetic effects when the particle size of Co_3O_4 is decreased [6]. In fact, Co_3O_4 synthesized by the hydrolysing method has T_N values varying from 32 to 17 K and 28 to 19 K for nanoparticles with size ranging from 37 to 15 nm [7]. Similar results were observed for Co_3O_4 nanoparticles synthesized by the conventional hydrothermal method, which presents particle diameter close to 30 nm [8]. A lower transition temperature (T_N ~15 K) was observed in Co_3O_4 nanoparticles with a diameter of 4 nm [9]. Some works described a superparamagnetic behaviour on the magnetic properties of Co_3O_4 nanoparticles and reported this effect with a blocking temperature of approximately 29 K in Co_3O_4 nanoparticles with diameters of 10-20 nm [6, 10, 11]. Such a superparamagnetic effect is unusual with the blocking temperature, T_B, immediately above T_N in the paramagnetic state [12]. Then, weak ferromagnetism can be observed at low temperature ($T < 5$ K) in Co_3O_4 nanoparticles, whose origin can be related to the superparamagnetic blocking state below T_B or the uncompensated surface spins and finite size in these oxides [5, 12, 13].

This dependence of the magnetic properties on the size of the Co_3O_4 particles has promoted several studies on the synthesis of this oxide by different chemical routes, such as sol-gel [6], solid-state thermal decomposition [14], and conventional [15] and microwave-assisted hydrothermal methods [16]. In the synthesis using both hydrothermal

methods, to obtain the single-phase Co_3O_4, an additional heat treatment is commonly necessary. Usually, these heat treatments are performed at temperatures of 200–500°C for 2-3 h [17, 18].

However, Zhou et al. [19] reported the synthesis of Co_3O_4 using a conventional hydrothermal method with no additional heat treatment. In this synthesis, the addition of hydrogen peroxide (H_2O_2) in the reactional medium promoted the formation of Co_3O_4 after the hydrothermal treatment at 150°C for 24 h. Other work reported the synthesis of Co_3O_4 particles using the hydrothermal method with no additional heat treatment and using H_2O_2 as oxidizing agent, where the conventional hydrothermal treatment was performed at 150°C for 12 h [20].

In conventional and microwave-assisted hydrothermal syntheses, the morphology and the size of Co_3O_4 depend on several parameters, such as the type of cobalt salts, solvent, solution pH, oxidizing agent, and reaction temperature and time [21]. Although the conventional hydrothermal synthesis requires a long period of synthesis, the microwave-assisted hydrothermal synthesis accelerates the reaction kinetics and increases the nucleation rate, which can reduce the reaction time [22]. A Co_3O_4 nanoplatelet was synthesized using cobalt acetate, sodium hydroxide, and citric acid as a precursor, with the microwave-assisted hydrothermal synthesis [23]. The hydrothermal treatment was performed at 200°C for 30 min under 1000 W. The obtained particles have an average diameter of approximately 123 nm and a thickness of 20 nm. In the literature, the synthesis methods can control the particle shape and size [17]. For example, both hydrothermal methods, with or without additional heat treatment, can produce particles with different morphologies and size, such as nanocubes [24], nanowires [25], and nanoflakes [26], and have shown that these characteristics affect the Co_3O_4 properties.

This work describes a simple and fast synthesis method to obtain Co_3O_4 nanoplates and nanocubes, which combines the advantages of a microwave-assisted hydrothermal method and the addition of urea or H_2O_2 in the reactional medium. This methodology does not require additional conventional heat treatment, and samples can be produced in only 10 min. The magnetic properties of these Co_3O_4 nanostructures were evaluated through magnetization measurements, and the effects of the shape and size on these properties were analysed.

2. Methods

The samples were prepared following two synthetic routes. In the first route, to obtain the Co_3O_4 nanoparticles, an aqueous solution of 0.8 mol/L of $Co(NO_2)_3$ (99%, Acros) was rapidly dropped into a solution of 0.65 mol/L of potassium hydroxide (KOH—99%, Sigma-Aldrich) under agitation. After the reaction, a light-brown-colored cobalt hydroxide precipitate was obtained and maintained under agitation for 30 min. Then, 50% in vol. of hydrogen peroxide (H_2O_2—29%, Synth) was utilized as the oxidizing agent [27]. The mixture was hydrothermally treated in a microwave reactor (Anton Paar, model Synthos 3000) at 220°C for 10 and 60 min; these samples are denoted as CH2-10 and CH2-60, respectively.

In the second route, a urea solution was used as the oxidizing agent. The ratio of urea : metal was maintained at 1 : 1. This solution was hydrothermally treated in the microwave reactor. In this case, the hydrothermal treatment was performed at 180°C during 10 and 60 min; these samples were denoted as CU-10 and CU-60, respectively. In both cases, the resulting product was collected, washed with deionized water and ethanol, and dried at 100°C overnight.

The final product was characterized by X-ray powder diffraction (XRD), using a Bruker D8 Focus X-ray Diffractometer, with CuK_α ($\lambda = 1.54056$ Å) radiation, an angular range of 15-70°, an angular step of 0.02°, and an exposure time of 5 s. The microstructure was evaluated by transmission electron microscopy (TEM), which images were taken in a Tecnai FEI equipment model G20. The samples were also characterized by Fourier transform infrared spectroscopy (FTIR), which was performed in Varian equipment model 640-IR. KBr was added to the samples and pressed in pellets to perform the transmittance measurements in the range of 400-2,000 cm^{-1}. Magnetic measurements were performed in a commercial superconducting quantum interference device (SQUID) magnetometer MPMS3 Quantum Design. These measurements were realized in field cooled (FC) and zero field cooled (ZFC) procedures, in the temperature range of 2-300 K with an applied magnetic field (H) up to 50 Oe. The hysteresis curves were obtained in a magnetic field (H) between $\pm 6T$, at 300 and 5 or 2 K.

3. Results and Discussion

Figure 1 shows the XRD results for the Co_3O_4 particles synthesized by hydrothermal treatment with H_2O_2 and urea as an oxidizing agent. Several parameters were studied to optimize synthesis conditions, such as the synthesis temperature and time. This result shows that except for the sample synthesized with urea by 10 min (CU-10), all the synthesis conditions promoted the Co_3O_4 phase formation, without impurity phases. All Bragg reflections in these X-ray patterns were identified as belonging to the cubic spinel system and matched with those reported by standard ICDD card no. 76-1802 (space group $Fd3\bar{m}$). These samples are single phase with no visible trace common secondary phases like CoO or $Co(OH)_2$. This result shows that it is possible to obtain Co_3O_4 using 10 min by microwave-assisted hydrothermal synthesis with no additional heat treatment.

The lattice parameters calculated from XRD data are approximately 0.808(5) nm for all samples; these values are listed in Table 1. These lattice parameters values are consistent with the data reported for Co_3O_4 [10]. The crystallite size, t, of all samples was estimated from XRD data using Scherrer's formula [28]

$$t = \frac{k\lambda}{B\cos\theta}, \quad (1)$$

where λ is the X-ray radiation wavelength, k is a Scherrer's constant, B is the full width at half maximum of the

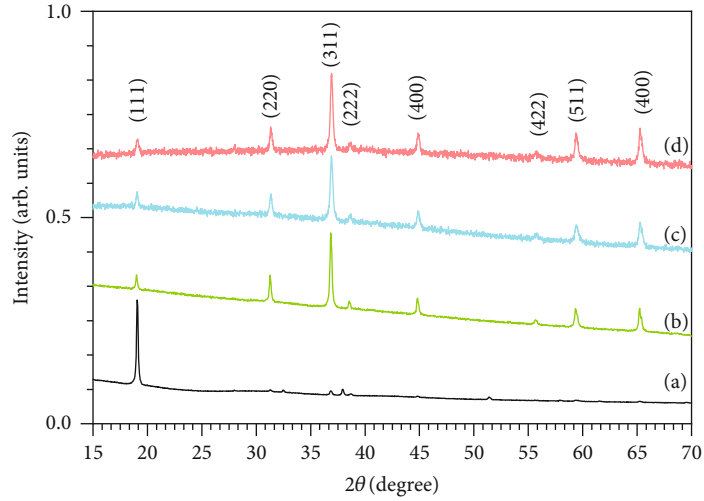

FIGURE 1: X-ray diffraction of Co_3O_4 particles that were hydrothermally synthesized with (a) urea at 180°C for 10 min (CU-10), (b) urea at 180°C for 60 min (CU-60), (c) KOH and 50% H_2O_2 at 220°C for 10 min (CH2-10), and (d) KOH and 50% H_2O_2 at 220°C for 60 min (CH2-60).

TABLE 1: Lattice parameters, crystallite size, and magnetic parameters calculated for CH2-10, CH2-60, and CU-60 samples.

	a	t	μ_{eff}	θ (K)	R^2
CH2-10	0.807	31.6	4.9	-89.0	0.9999
CH2-60	0.808	41.0	5.3	-101	0.9999
CU-60	0.808	34.2	—	—	—

diffraction peaks (in radians), and θ is the Bragg angle. The obtained t values for the crystallite sizes are 32, 41, and 34 nm for samples CH2-10, CH-60, and CU-60, respectively. Those results are consistent with crystallite values of 15-65 nm listed in literature for Co_3O_4 synthesized by hydrothermal method [13].

Figure 2 exhibits the FTIR spectra for all the synthesized samples in this work. The FTIR spectra of CH2-60, CH2-10, and CU-10 revealed a similar behaviour; they display two intense bands at 575 cm^{-1} (υ_1) and 665 cm^{-1} (υ_2), which are assigned to the metal-oxygen band and confirm the formation of the desired Co_3O_4 spinel phase. The υ_1 vibration is attributed to the intrinsic stretching vibration of Co^{3+} at the octahedral site, and the υ_2 band is assigned to stretching vibration of Co^{2+} in the tetrahedral site in the spinel lattice [14, 29–32]. The low intense band near 1400 cm^{-1} can be attributed to υ_1 vibration of dioxide carbon due to traces of atmospheric CO_2, which can be adsorbed during the measurements [30]. The band close to ~1600 cm^{-1} is assigned to the H-O stretching vibration of interaction through H bonds [29–31].

A uniform plate-like shape of the samples CH2-60 can be observed by TEM images (see Figure 3) that present a size distribution of ~70 nm. The CH2-10 TEM image revealed the particle size smaller than 10 nm. The cube-like shape Co_3O_4 nanoparticles were observed in the TEM images of CU-60 with a mean particle size of 35-58 nm. This result indicates that for the sample synthesized with H_2O_2, the particle morphology is not affected by the time increment from 10 to 60 min, but the time of synthesis promoted an increase in the particle size. The oxidizing agent (H_2O_2 or urea) also modifies the nanoparticle shape from plate to cube.

The temperature dependence of magnetic susceptibility, $\chi(T)$, of Co_3O_4 samples is shown in Figure 4. The $\chi(T)$ curves for all the samples exhibit a cusp at T_P ~22 and 24 K for the CH2-10 and CH2-60, respectively, and 36 K for CU-60. A clear bifurcation of the ZFC and FC curves is observed below T_P for all the samples; such behaviour is related to a superparamagnetic blocking in magnetic nanoparticle system [4, 6, 13]. In fact, the Co_3O_4 bulk presents a paramagnetic behaviour at high temperatures and a ferromagnetic ordering below T_N (near 30-40 K) [6]. In these bulk samples, ZFC and FC curves below T_P are almost coincident, but a decrease in Co_3O_4 particle size implies a reduction in T_N values, and a remarkable bifurcation of ZFC and FC curves appears [6, 11]. Similar behaviour is observed through $\chi(T)$ measurements for Co_3O_4 samples at $T > T_P$, although a comparison among Figures 4(a), 4(b), and 4(c) shows a rather different behaviour below T_P. In fact, $\chi(T)$ increased by one order of magnitude for CH2-10 and CH2-60 in comparison with $\chi(T)$ curve of sample CU-60. The curves in Figure 4(d) for samples CH2-10 and CH2-60 present a sharp and low intense cusp at T_P, and FC curves drastically increase below this cusp. A similar behaviour was observed in particles with a size of 17-37 nm, whereas the observed particles sizes of CH2-10 and CH2-60 are approximately 10 and 60 nm, respectively.

To verify the peak temperature, we plotted $\partial M/\partial T$ versus temperature (not shown) and find T_N ~21 K for CH2-10 and T_N ~22 K for CH2-60 sample. Figure 4(a) shows the temperature dependence of magnetic susceptibility for CU-60 sample, which presents a broader cusp at T_P ~36 K. The first derivative of these data reveals T_{Max}~28 K, which is different from T_P, but is consistent with the literature [6]. This significant change in the $M(T)$ curve is attributed to

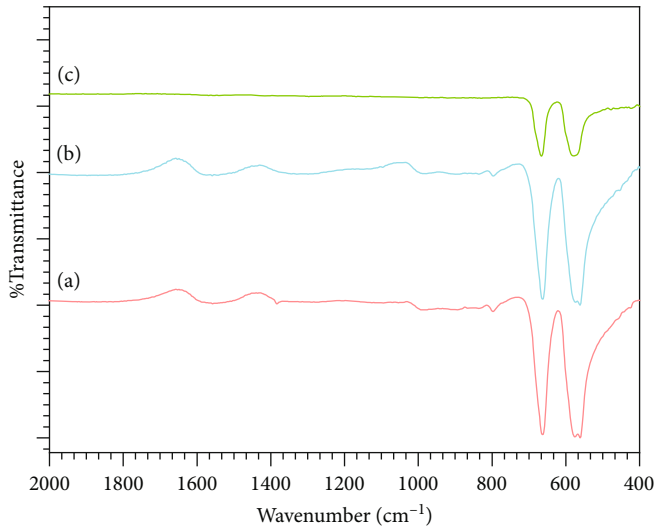

FIGURE 2: FTIR spectra of Co_3O_4 nanoparticles that were synthesized at 220°C with KOH during (a) 60 min (CH2-60) and (b) 10 min (CH2-10) and (c) Co_3O_4 nanoparticles synthesized at 180°C at 60 min with urea (CU-60).

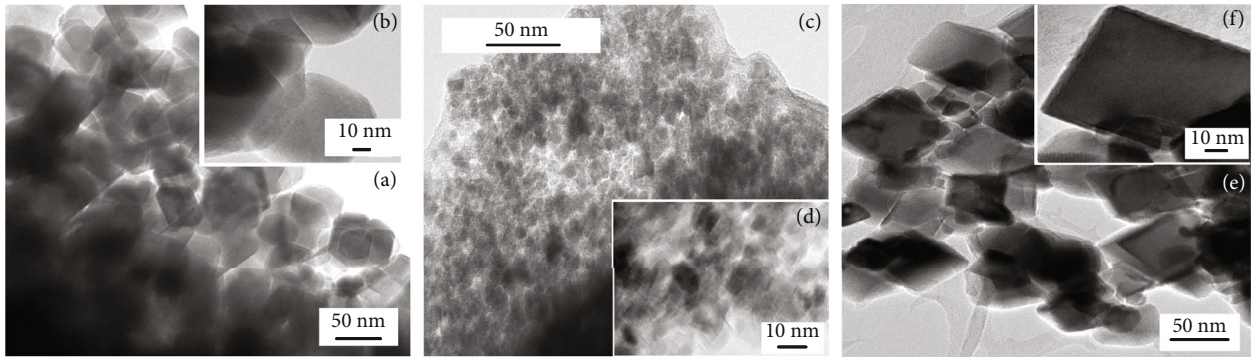

FIGURE 3: TEM images of Co_3O_4 nanoparticles synthesized with KOH and H_2O_2 at 220°C during (a, b) 60 min (CH2-60) and (c, d) 10 min (CH2-10) and (e, f) nanocubes synthesized with urea at 180°C during 60 min (CU-60).

changes in the size and shape of the Co_3O_4 particles. It is important to notice that the magnetic behaviour of all the samples indicates characteristics that can be addressed to nanoparticle magnetism. In fact, some author relates these features with the presence of an unusual superparamagnetic effect [12]. Because the T_P values appear to be independent of the applied magnetic field, at $T > T_P$, it is believed that the magnetization curves of Co_3O_4 nanoparticles display a typical paramagnetic behaviour. This result is different from those reported results of other ferromagnetic nanoparticles, whose T_P is dependent on the applied magnetic fields. At temperatures immediately below T_P, a sudden increase in $M(T)$ is observed for the Co_3O_4 particles, which appears to correspond to a blocked state as observed in superparamagnetic particles in the literature [12]. The magnetic susceptibility was analysed using the Curie-Weiss equation

$$\frac{1}{\chi} = \frac{T-\theta}{C}, \tag{2}$$

where θ is the Weiss temperature and $C = N\mu_{eff}^2/3k_B$, where C is the Curie constant, N is the calculated number of Co_3O_4 per 1 g and is the effective magnetic moment, and k_B is the Boltzmann constant. The fits are listed in Figure 5, and the estimated values are shown in Table 1. μ_{eff}^2 is approximately 4.9 for CH2-10 and approaches the experimentally observed value for bulk Co_3O_4 [5, 10], and for CH2-60, μ_{eff}^2 is close to 5.3. Similar results were reported in the literature for Co_3O_4 samples [7]. This variation of values can be related to a possibly disordered distribution of Co^{2+} and Co^{3+} ions in the metallic sites A and B of the inverse spinel structure or the inaccuracy of Curie-Weiss law to describe the contribution of the $4F_9/2$ ground state of Co^{2+}.

The Co_3O_4 samples were also characterized by $M \times H$ using magnetic field that varied from -6T to 6T at 300 and 5 or 2 K. The $M \times H$ curves for samples CH2-10 and CH2-60 (Figure 6) at 300 K present linear field dependence with zero coercive fields and remnant magnetization; such linear dependence is a feature characteristic of paramagnetic behaviour expected for these samples. At 5 K, these curves reveal a

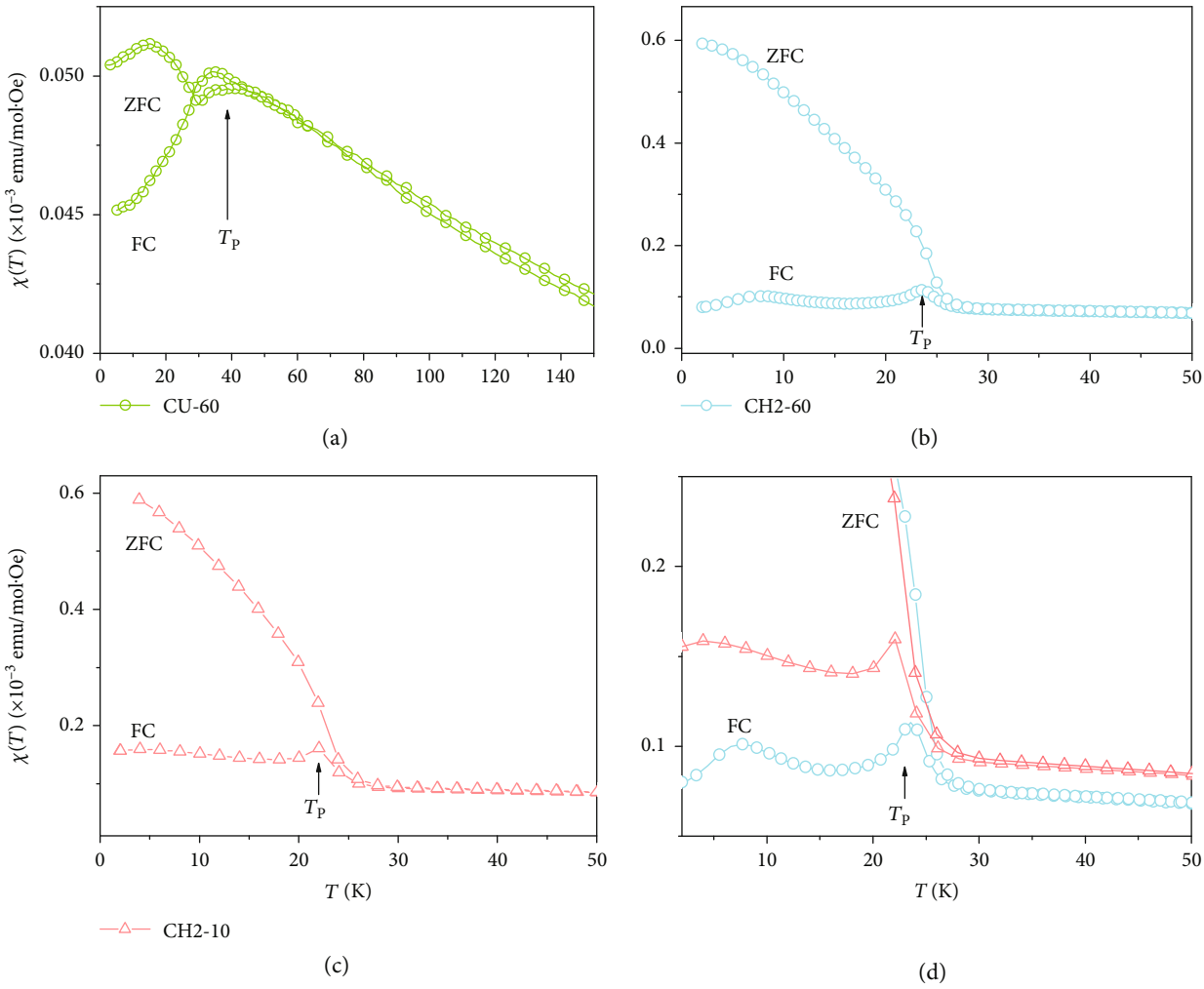

Figure 4: Temperature dependence of magnetic susceptibility in the ZFC and FC process at $H = 50$ Oe for Co_3O_4 nanoparticles that were synthesized with (a) urea at 180°C during 60 min (CU-60), (b) H_2O_2 at 220°C for 60 min (CH2-60), and (c) H_2O_2 at 220°C for 10 min (CH2-10). (d) A comparison of magnetization versus temperature curves obtained for CH2-60 and CH2-10 samples.

hysteresis loop with symmetric coercive field (H_c) ~28 kOe and remnant magnetization (M_r) 0.042 emu/g for CH2-60 and H_c ~20 kOe and M_r 0.037 emu/g for CH2-10 sample. Similar hysteretic behaviour is also observed in Co_3O_4 nanoparticles (10 nm) in the literature that indicates weak ferromagnetism and can be related to the uncompensated surface spins and expected superparamagnetic blocked state below T_P [4, 13].

Different $M \times H$ curves were observed for CU-60 samples (see Figure 6), which present an almost linear behaviour at 300 or 2 K and a weak hysteresis loop with symmetric H_c ~99 and ~51 kOe and M_r ~3.66×10^{-4} at 300 K and 1.89×10^{-4} emu/g at 2 K. In addition, there is no saturation in the maximum field applied, which has been related to a notably weak ferromagnetic nature [32]. The $M \times H$ curves present a large coercivity near 600 Oe, as shown in Figure 6. These results show the strong effect of the particle shape and size on the magnetic properties of Co_3O_4. It should be observed that most hydrothermal synthesis performs additional low temperature heat treatment (~300°C) to obtain Co_3O_4 [33]. In this work, we have used a fast one-step synthesis procedure to synthesize the Co_3O_4, and we observed interesting magnetic properties, which seem to be related to the morphology and size of these Co_3O_4 nanoparticles.

4. Conclusions

Nanoplates and nanocubes of Co_3O_4 were produced by a fast-hydrothermal synthesis using temperatures of 180-220°C. Different morphologies and sizes are related to the synthesis time and oxidizing agent (urea and H_2O_2). The X-ray diffraction results revealed that all samples are single phase, with a crystallite size of 32, 41, and 34 nm for CH2-10, CH-60, and CU-60 samples, respectively. TEM images showed Co_3O_4 nanoparticles with a plate and cubic shapes with sizes of 10 to 70 nm. Based on the ZFC/FC magnetic measurements, we observed the effect of the size and morphology of the particles on the magnetic curves of these samples. Co_3O_4 nanoplates present a decrease in T_P temperatures with a decrease of the particle size. Also, the samples exhibit weak ferromagnetism, which is attributed to the uncompensated surface spins of particles and the presence of an unusual superparamagnetic state. The cube samples present lower $M(T)$ magnitude, and $M \times H$

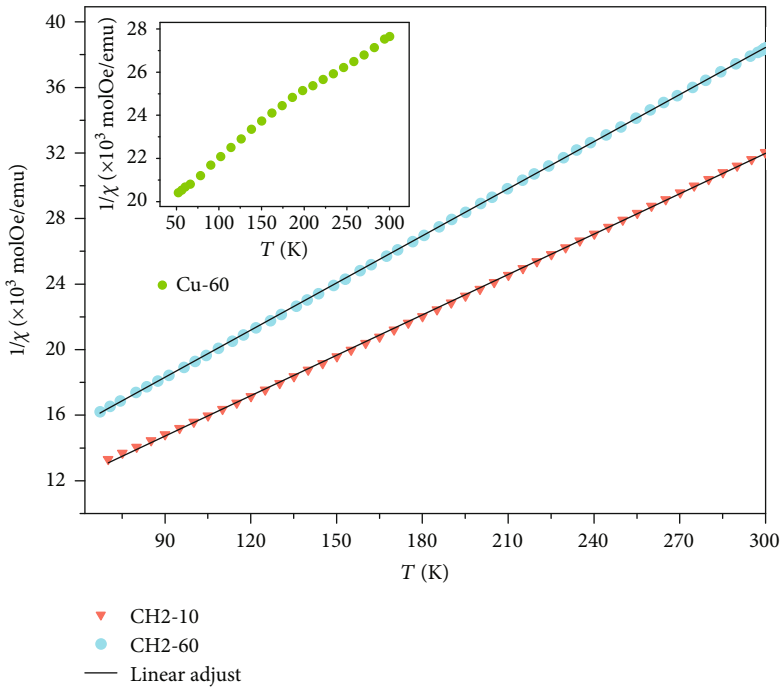

Figure 5: Inverse magnetic susceptibility versus temperature for Co_3O_4 nanoparticles CH2-10 (red triangle), and CH2-60 (blue circle), the black line show the linear fit performed in these curves. The inset shows the Inverse magnetic susceptibility for the CU-60 sample (green circle).

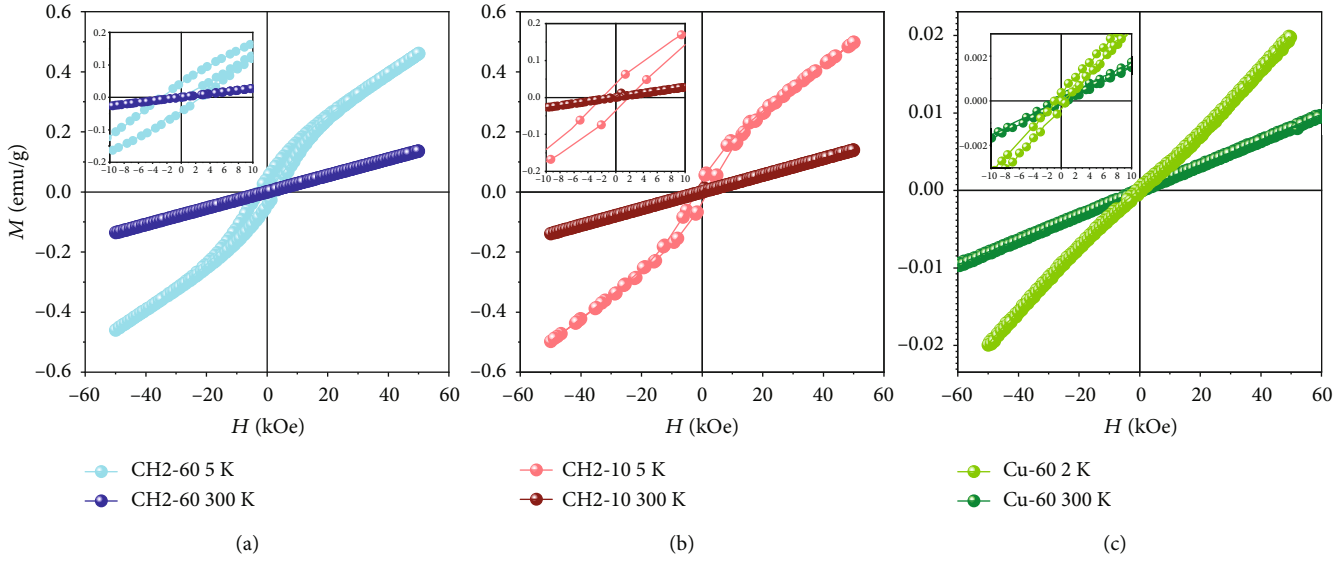

Figure 6: $M \times H$ curves for the samples synthesized at 220°C during (a) 60 min and (b) 10 min with H_2O_2 and synthesized at 180°C during (c) 60 min with urea.

measurements showed that these nanoparticles present a weak ferromagnetic behaviour at room temperature. These results showed that it is possible to control the magnetic properties of Co_3O_4 with varying synthesis conditions using the one-step microwave-assisted hydrothermal method.

Data Availability

The data used to support the findings of this study are available from the corresponding author upon request.

Conflicts of Interest

The authors declare that there is no conflict of interest regarding the publication of this paper literature.

Acknowledgments

The authors gratefully acknowledge the Multiuser Central Facilities at UFABC for the experimental support (XRD, SEM, and SQUID). Additionally, the authors acknowledge

the financial support provided by CAPES and FAPESP (grant no. 2016/03575-2 and no. 2019/06004-4).

Supplementary Materials

This document presents additional scanning electron microscopy images of Co_3O_4 nanoparticles (CH2-10 and CH2-60). Also, additional magnetic graphics show (a) the magnetic susceptibility as a function of temperature for all the samples, (b) the inverse of susceptibility versus temperature with the linear fitting to obtain the effective magnetic moment of Co ions and (c) the hysteretic loop obtained at different temperatures for all sample. *(Supplementary Materials)*

References

[1] Y. Wang, B. Wang, F. Xiao et al., "Facile synthesis of nanocage Co_3O_4 for advanced lithium-ion batteries," *Journal of Power Sources*, vol. 298, pp. 203–208, 2015.

[2] S. Vetter, S. Haffer, T. Wagner, and M. Tiemann, "Nanostructured Co_3O_4 as a CO gas sensor: temperature-dependent behavior," *Sensors and Actuators B: Chemical*, vol. 206, pp. 133–138, 2015.

[3] S. Sun, X. Zhao, M. Yang, L. Ma, and X. Shen, "Facile and eco-friendly synthesis of finger-like Co_3O_4 nanorods for electrochemical energy storage," *Nanomaterials*, vol. 5, no. 4, pp. 2335–2347, 2015.

[4] Y. Ichiyanagi and S. Yamada, "The size-dependent magnetic properties of Co_3O_4 nanoparticles," *Polyhedron*, vol. 24, no. 16-17, pp. 2813–2816, 2005.

[5] W. L. Roth, "The magnetic structure of Co_3O_4," *Journal of Physics and Chemistry of Solids*, vol. 25, no. 1, pp. 1–10, 1964.

[6] P. Dutta, M. S. Seehra, S. Thota, and J. Kumar, "A comparative study of the magnetic properties of bulk and nanocrystalline Co_3O_4," *Journal of Physics: Condensed Matter*, vol. 20, no. 1, article 015218, 2007.

[7] A. K. Sarfraz and S. K. Hasanain, "Size dependence of magnetic and optical properties of Co_3O_4 nanoparticles," *Acta Physica Polonica A*, vol. 125, no. 1, pp. 139–144, 2014.

[8] H. T. Zhu, J. Luo, J. K. Liang et al., "Synthesis and magnetic properties of antiferromagnetic Co_3O_4 nanoparticles," *Physica B: Condensed Matter*, vol. 403, no. 18, pp. 3141–3145, 2008.

[9] D. A. Resnick, K. Gilmore, Y. U. Idzerda et al., "Magnetic properties of Co_3O_4 nanoparticles mineralized in *Listeria innocua* Dps," *Journal of Applied Physics*, vol. 99, no. 8, article 08Q501, 2006.

[10] F. Moro, S. V. Yu Tang, F. Tuna, and E. Lester, "Magnetic properties of cobalt oxide nanoparticles synthesised by a continuous hydrothermal method," *Journal of Magnetism and Magnetic Materials*, vol. 348, pp. 1–7, 2013.

[11] L. He, C. Chen, N. Wang, W. Zhou, and L. Guo, "Finite size effect on Néel temperature with Co_3O_4 nanoparticles," *Journal of Applied Physics*, vol. 102, no. 10, article 103911, 2007.

[12] V. Bisht and K. P. Rajeev, "Unusual superparamagnetic behavior of Co3O4 Co3O4 nanoparticles," *RSC Advances*, vol. 5, pp. 46705–46710, 2015.

[13] G. Anandha Babu, G. Ravi, Y. Hayakawa, and M. Kumaresavanji, "Synthesis and calcinations effects on size analysis of Co_3O_4 nanospheres and their superparamagnetic behaviors," *Journal of Magnetism and Magnetic Materials*, vol. 375, pp. 184–193, 2015.

[14] A. D. Khalaji, R. Rahdaria, F. Gharib, J. S. Matalobos, and D. Das, "Preparation and characterization of Co3O4 nanoparticles by solid state thermal decomposition of cobalt (II) macrocyclic Schiff base complexes," *Journal of Ceramic Processing Research*, vol. 16, pp. 486–489, 2015.

[15] W. E. Mahmoud and F. A. Al-Agel, "A novel strategy to synthesize cobalt hydroxide and Co_3O_4 nanowires," *Journal of Physics and Chemistry of Solids*, vol. 72, no. 7, pp. 904–907, 2011.

[16] C. Sun, X. Su, F. Xiao, C. Niu, and J. Wang, "Synthesis of nearly monodisperse Co_3O_4 nanocubes via a microwave-assisted solvothermal process and their gas sensing properties," *Sensors and Actuators B: Chemical*, vol. 157, no. 2, pp. 681–685, 2011.

[17] L.-H. Ai and J. Jiang, "Rapid synthesis of nanocrystalline Co_3O_4 by a microwave-assisted combustion method," *Powder Technology*, vol. 195, no. 1, pp. 11–14, 2009.

[18] B. Niu, L. Man, and J. Wang, "Microwave hydrothermal synthesis of nano Co_3O_4 with various morphologies," *Integrated Ferroelectrics*, vol. 129, no. 1, pp. 181–187, 2011.

[19] K. Zhou, J. Liu, P. Wen, Y. Hu, and Z. Gui, "Morphology-controlled synthesis of Co_3O_4 by one step template-free hydrothermal method," *Materials Research Bulletin*, vol. 67, pp. 87–93, 2015.

[20] X. C. Song, X. Wang, Y. F. Zheng, R. Ma, and H. Y. Yin, "Synthesis and electrocatalytic activities of Co_3O_4 nanocubes," *Journal of Nanoparticle Research*, vol. 13, no. 3, pp. 1319–1324, 2011.

[21] Y. P. Yang, K. L. Huang, R. S. Liu, L. P. Wang, W. W. Zeng, and P. M. Zhang, "Shape-controlled synthesis of nanocubic Co_3O_4 by hydrothermal oxidation method," *Transactions of Nonferrous Metals Society of China*, vol. 17, no. 5, pp. 1082–1086, 2007.

[22] B. L. Hayes, *Microwave Synthesis: Chemistry at the Speed of Light*, CEM Matthews NC, 2006.

[23] R. Al-Tuwirqi, A. A. Al-Ghamdi, N. A. Aal, A. Umar, and W. E. Mahmoud, "Facile synthesis and optical properties of Co_3O_4 nanostructures by the microwave route," *Superlattices and Microstructures*, vol. 49, no. 4, pp. 416–421, 2011.

[24] M. Kang and H. Zhou, "Facile synthesis and structural characterization of Co_3O_4 nanocubes," *AIMS Materials Science*, vol. 2, no. 1, pp. 16–27, 2015.

[25] S. K. Meher and G. R. Rao, "Effect of microwave on the nanowire morphology, optical, magnetic, and pseudocapacitance behavior of Co_3O_4," *The Journal of Physical Chemistry C*, vol. 115, no. 51, pp. 25543–25556, 2011.

[26] S. Chen, Y. Zhao, B. Sun et al., "Microwave-assisted synthesis of mesoporous Co_3O_4 nanoflakes for applications in lithium ion batteries and oxygen evolution reactions," *ACS Applied Materials & Interfaces*, vol. 7, no. 5, pp. 3306–3313, 2015.

[27] M. Miclau, K. Bokinala, and N. Miclau, "Low-temperature hydrothermal synthesis of the three-layered sodium cobaltite P3-Na_xCoO_2 ($x \sim 0.60$)," *Materials Research Bulletin*, vol. 54, pp. 1–5, 2014.

[28] P. Scherrer, "Nachrichten von der gesellschaft der wissenschaften zu göttingen," *Mathematisch-Physikalische Klasse*, vol. 2, pp. 98–100, 1918.

[29] T. O. Ahmadov, Z. Durmus, A. Baykal, and H. Kavas, "A simple approach for the synthesis of Co_3O_4 nanocrystals," *Inorganic Materials*, vol. 47, no. 4, pp. 426–430, 2011.

[30] T. Ozkaya, A. Baykal, M. S. Toprak, Y. Koseoğlu, and Z. Durmuş, "Reflux synthesis of Co_3O_4 nanoparticles and its magnetic characterization," *Journal of Magnetism and Magnetic Materials*, vol. 321, no. 14, pp. 2145–2149, 2009.

[31] T. Ozkaya, A. Baykal, Y. Koseoğlu, and H. Kavas, "Synthesis of Co_3O_4 nanoparticles by oxidation-reduction method and its magnetic characterization," *Open Chemistry*, vol. 7, no. 3, pp. 410–414, 2009.

[32] P. Sahoo, H. Djieutedjeu, and P. F. P. Poudeu, "Co_3O_4 nanostructures: the effect of synthesis conditions on particles size, magnetism and transport properties," *Journal of Materials Chemistry A*, vol. 1, no. 47, pp. 15022–15030, 2013.

[33] S. Shafiu, A. Baykal, H. Sözeri, and M. S. Toprak, "Triethanolamine assisted hydrothermal synthesis of superparamagnetic Co_3O_4 nanoparticles and their characterizations," *Journal of Superconductivity and Novel Magnetism*, vol. 27, no. 9, pp. 2117–2122, 2014.